---

**Article:**
Salt, S.J., Weldeyesus, A.G., Gilbert, M. orcid.org/0000-0003-4633-2839 et al. (1 more author) (2023) Layout optimization of pin-jointed truss structures with minimum frequency constraints. Engineering Optimization, 55 (8). pp. 1403-1421. ISSN 0305-215X

https://doi.org/10.1080/0305215X.2022.2086539

---

Engineering Optimization

ISSN: (Print) (Online) Journal homepage: https://www.tandfonline.com/loi/geno20

# Layout optimization of pin-jointed truss structures with minimum frequency constraints

S. J. Salt, A. G. Weldeyesus, M. Gilbert & J. Gondzio

**To cite this article:** S. J. Salt, A. G. Weldeyesus, M. Gilbert & J. Gondzio (2022): Layout optimization of pin-jointed truss structures with minimum frequency constraints, Engineering Optimization, DOI: 10.1080/0305215X.2022.2086539

**To link to this article:** https://doi.org/10.1080/0305215X.2022.2086539



Published online: 17 Jul 2022.

ENGINEERING OPTIMIZATION
https://doi.org/10.1080/0305215X.2022.2086539

Taylor & Francis
Taylor & Francis Group



# Layout optimization of pin-jointed truss structures with minimum frequency constraints

S. J. Salt [a], A. G. Weldeyesus [b], M. Gilbert [c] and J. Gondzio [b]

[a]Rolls-Royce plc, Derby, UK; [b]School of Mathematics and Maxwell Institute, The University of Edinburgh, Edinburgh, UK; [c]Department of Civil and Structural Engineering, University of Sheffield, Sheffield, UK

**ABSTRACT**

Controlling the frequency response of an engineering component or structure is important in the aerospace and automotive sectors and is a key consideration when seeking a new and more efficient design for a given component. In this contribution, the standard truss layout optimization procedure is modified to incorporate semidefinite constraints to limit the minimum value of the first natural frequency. Since this increases the computational expense and reduces the scale of the problem that can be solved, a bespoke algorithm incorporating an adaptive 'member adding' procedure is proposed and applied to a number of benchmark example problems. It is demonstrated that this allows problems to be solved with relatively fine numerical discretization, allowing modified structures with an acceptable minimum first natural frequency response to be successfully identified.

**ARTICLE HISTORY**
Received 26 June 2021
Accepted 25 March 2022

**KEYWORDS**
Layout optimization; topology optimization; truss structures; frequency constraints

## 1. Introduction

In the design of modern engineering components, many considerations need to be taken into account including safety, cost, weight and manufacturability. The most prominent of these is safety, taking account of the regime of applied stresses to be sustained over the life of the component. Safety is influenced by the properties of the material employed, which may change as the design evolves. Additionally, when considering structures that include slender elements in compression, it is necessary to check for buckling instability to ensure safety is maintained. Another key parameter in the aerospace sector is the harmonic frequency of a structure. This should lie outside the frequency bands of surrounding components. Should a fundamental frequency of one component (*e.g.* a bracket) overlap with those of its attached neighbours, then resonance in the component may occur, also referred to as forced vibration. Forced vibration and resonance can then lead to High Cycle Fatigue (HCF) in the component, affecting its serviceable life and reducing its time to failure. It should be noted that a component may exhibit multiple resonant frequencies, each corresponding to a mode of vibration; repeated exposure to these frequencies may reduce the life of the component. However, this phenomenon is beyond the scope of the current contribution. Considering component manufacture, it is important to note that traditional manufacturing methods may limit the design freedom available; however, in the present contribution, it is assumed that Additive Layer Manufacturing (ALM) methods are available. The use of ALM means that complex truss forms can potentially be fabricated, beyond the scope of traditional subtractive manufacturing methods.

**CONTACT** M. Gilbert m.gilbert@sheffield.ac.uk

There have been numerous recorded HCF related incidents. A notable example led to the loss of British Midland flight #92 in 1989 (Cooper 1989). This was initiated by the failure of a fan blade on one of the two CFM International S.A. CFM56-3 turbofan engines. A single blade failed owing to the coupling of a torsional–flexural transient and a non-synchronous oscillation, leading to rapid reduction of the HCF life of the blade. The blade was subsequently released, causing high levels of vibration in the engine and aircraft, contributing to the loss of the aircraft upon attempting an emergency landing at East Midlands Airport in the UK.

Given the potentially catastrophic consequences of failure, the design optimization of components with stress and frequency constraints has been of interest for many years. Forced vibration problems can be avoided by (a) redesigning the component being analysed, (b) redesigning the stimuli to change its frequency characteristics, and/or (c) introducing a damping mechanism into the system. The most straightforward of these options is often (a), redesigning a component to move its fundamental frequencies away from those where resonance may occur. This may be achieved, for example, by adding stiffening ribs to the part or strategically increasing the volume of material.

Computer aided methods have been employed to treat such problems, largely focusing upon the use of topology optimization in works such as Bendsøe and Sigmund (2003), where links can be formed between discrete and continuum structures (Achtziger 1999). Additionally, Du and Olhoff (2007) formulated simple and multiple eigenfrequency optimization techniques for linear elastic structures without damping. The present contribution will focus upon the design of truss structures that are attractive when there is significant available design freedom. In practice, it is rare that the available design freedom is fully exploited, usually due to limitations associated with the manufacturing method involved. However, ALM allows the available design freedom to be exploited to a much greater extent than when traditional subtractive manufacturing methods are employed. Since the ground structure method was first introduced by Dorn, Gomory, and Greenberg (1964) to solve plastic truss design problems, layout optimization has provided an effective means of identifying the most efficient arrangement of elements (also referred to herein as 'members' or 'bars') to form a truss structure. This methodology has been well used to identify minimum volume truss structures (Dorn, Gomory, and Greenberg 1964; Hemp 1973; Gilbert and Tyas 2003; Smith *et al.* 2016) using Linear Programming (LP) and member adding (column generation) to solve single load case problems efficiently. These methods have been further extended by Pritchard, Gilbert, and Tyas (2005) and Sokół (2014) to include application to multiple load cases; to keep the underlying layout optimization problem formulation reasonably simple, the present contribution will focus on single load case problems with a single specified minimum frequency, usually chosen so as to lie away from the frequencies of any sources of excitation. However, frequency analysis is a nonlinear problem and so semidefinite programming (SDP) must be used to treat the constraints.

SDP is a subset of convex optimization and aims to minimize a linear function subject to the constraint that an affine combination of symmetric matrices is positive semidefinite. SDP has been applied to the optimization of truss structures previously by Ben-Tal and Nemirovski (1997), and later Kanno (2018) used SDP to produce structures that were robust against uncertainty in the loading, and Giniünaité (2015) applied SDP to identify minimum mass structures. A number of solvers are available that are capable of treating semidefinite problems of varying complexity: `fminsdp` (Thore 2018); MOSEK (v8+) (MOSEK ApS 2017); PENLAB (Fiala, Kočvara, and Stingl 2013) and CVX (Grant and Boyd 2014) are a few examples. However, a bespoke approach is required when combining generative truss design with optimization for frequency constraints.

Frequency optimization belongs to the field of eigenvalue optimization in mathematics, which has been studied extensively by the mathematical programming community: Fox and Kapoor (1970) adopted a feasibility approach to solve the underlying semidefinite programming problem, Grandhi and Venkayya (1988) and Khot (1985) used the optimality criteria method and Kaveh and Ghazaan (2016) used non-smooth optimization to perform size optimization of existing truss structures to meet certain frequency requirements. Additionally, Achtziger and Kočvara (2007) used SDP to solve similar problems, and Aroztegui *et al.* (2011) developed a feasible direction algorithm for SDP

in order to maximize the fundamental frequencies based upon simple fully connected ground structures. Considering optimization of frequency in isolation, Azad *et al.* (2018) assessed the simultaneous size and geometry optimization of steel structures under excitation using the 'big bang–big crunch' algorithm, with mixed results when considering the optimum solutions, whilst Taheri and Jalili (2016) and Tejani *et al.* (2018) used other meta-heuristic methods to impose frequency constraints in truss optimization problems.

In many of these studies, the design variable was treated as continuous but the number and arrangement of the variables were assumed to be finite and arrived at by utilizing the most efficient members from a pre-defined ground structure. By contrast, in the present article an alternative methodology is proposed in which standard equilibrium constraints are supplemented by semidefinite constraints to enable problems involving both frequency and strength considerations to be tackled. The ground structure method is employed to provide a large search space, with an adaptive member adding algorithm used to reduce the associated computational burden significantly. In the interests of simplicity, buckling instability and other issues are not considered explicitly in this contribution, though would need to be checked prior to, for example, usage in a qualified aerospace application.

This article is organized as follows: Section 2 describes the basic formulations relevant to the frequency problem at hand, with examples used to illustrate limitations; Section 3 then proposes a new formulation that is significantly more computationally efficient; the new formulation is then applied to various example problems in Section 4; and conclusions are drawn in Section 5.

## 2. Basic formulations

### 2.1. Truss layout optimization formulation

Ground structure-based layout optimization begins with the definition of a design domain, the volume of space in which the optimized structure can reside, with materials, loads and supports then also prescribed to describe the problem fully, see Figure 1(a). The objective is to arrive at a structure of minimum volume, and hence mass, whilst maintaining structural integrity. With a Cartesian grid, the design domain is populated with a predefined number of nodes $n$ in the $x$- and $y$-directions (also in the $z$-direction for 3D problems). It is then joined with $m$ potential connections, or elements, such that each node is connected to every other node in the domain to form a ground structure, as in Figures 1(b) and 1(c). Herein, each example will employ a number of nodes expressed in terms of the number of nodal divisions, *e.g.* referring to Figure 1(b), the domain has $4 \times 2$ nodal divisions, with 4 divisions and 5 nodes in the $x$-direction and 2 divisions and 3 nodes in the $y$-direction, giving 15 nodes in total. Constraints are introduced to ensure equilibrium is enforced at nodes, and to ensure that the cross-sectional area of each element is both a positive number and is sufficiently large to carry the internal forces, given the limiting stress of the material. The plastic single load case formulation can be written as (after Dorn, Gomory, and Greenberg 1964):

$$\begin{aligned} \min_{\boldsymbol{a},\boldsymbol{q}} \quad & V = \mathbf{l}^{\mathrm{T}}\boldsymbol{a} \\ \text{s.t.} \quad & \begin{cases} \mathbf{B}\boldsymbol{q} = \mathbf{p}, & \\ -\sigma^{-}a_i \le q_i \le \sigma^{+}a_i, & \forall\, i \\ a_i \ge 0, & \forall\, i, \end{cases} \end{aligned} \tag{1}$$

where $V$ is the total volume of the structure; $\mathbf{l}$ is a vector of individual element lengths $\{l_1, l_2, \ldots, l_m\}$; $\boldsymbol{a}$ is a vector containing element cross-sectional areas $\{a_1, a_2, \ldots, a_m\}$; $\mathbf{B}$ is a suitable ($2n \times m$ or $3n \times m$) equilibrium matrix containing direction cosines (for 2D or 3D problems); $\boldsymbol{q}$ is a vector of element axial forces, $\boldsymbol{q} = \{q_1, q_2, \ldots, q_m\}$, where $q_i$ is the force in element $i$; $\mathbf{p}$ is a vector of applied loads and $\mathbf{p} = \{p_1^x, p_1^y, p_1^z, p_2^x, p_2^y, p_2^z, \ldots, p_n^z\}$ where $p_j^x, p_j^y, p_j^z$ are the $x$-, $y$- and $z$-direction components of the load applied to node $j$ ($j = 1, \ldots, n$). Finally $\sigma^+$ and $\sigma^-$ are, respectively, the limiting tensile and

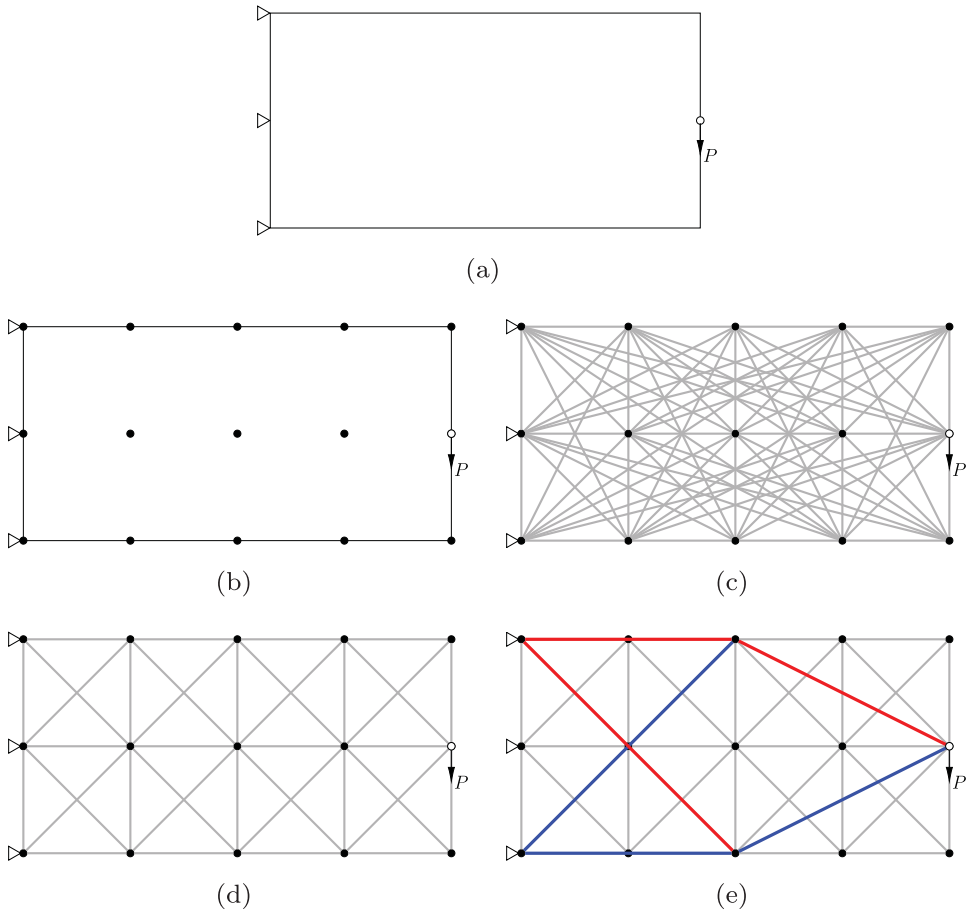


**Figure 1.** Steps in layout optimization: (a) definition of the problem domain and boundary conditions; (b) domain populated with equally spaced nodes; (c) each node is connected to every other node in the domain to form a fully connected ground structure or (d) each node is connected only to neighbouring nodes to form a minimally connected ground structure; and (e) the resulting optimized layout using a member adding algorithm (red and blue bars indicate those in tension and compression, respectively [online only]).

compressive stresses that can be sustained by the material. Problems of this nature may be solved using linear programming.

Employing a fully connected ground structure of this type is computationally expensive, with the problem comprising $n(n-1)/2$ potential connections for a domain, where $n$ is the total number of nodes. The majority of the connections will have an area equal or close to zero following the optimization and so do not contribute to the final structure. This issue may be alleviated by applying the adaptive 'member adding' method proposed by Gilbert and Tyas (2003), which is a customized column generation technique. With this method, nodes in the initial ground structure are only connected to their immediate neighbours, Figure 1(d), instead of to every other node in the domain, Figure 1(c). An iterative process is then used, with elements added to the current ground structure from the list of potential connections. Newly added elements are introduced into the solution using the Michell–Hemp criterion (2), which specifies limits on the virtual strain ($\varepsilon$) experienced by each potential element ($i$), given a prescribed limiting stress ($\sigma$):

$$-\frac{1}{\sigma^-} \leq \varepsilon_i \leq \frac{1}{\sigma^+}, \quad i = 1, \ldots, m. \tag{2}$$

In the parlance of the column generation method (Gondzio and Sarkissian 1996; Desrosiers and Lübbecke 2005; Gondzio, González-Brevis, and Munari 2013), new columns are added to the LP constraint matrix **B** in (1). At the end of each iteration, potential connections are ranked, with those most violating the criteria then added for use in the next iteration. Once there are no potential connections violating the criteria remaining, the algorithm terminates. The solution obtained shown in Figure 1(e) is provably optimal, with the computed volume the same as that obtained using a fully connected ground structure.

### 2.2. General eigenvalue equation

Consider a truss structure consisting of $m$ elements connecting a pre-determined set of $n$ nodes. A large external force $P$ is applied to a specific node, with internal forces transmitted through the structure, resulting in small displacements at each node; this may be considered to be a static problem. To take account of the vibration characteristics of the structure, it is necessary to consider the following dynamic problem derived from the equation of motion:

$$\mathbf{K}\{\boldsymbol{u}\} + \mathbf{M}\{\ddot{\boldsymbol{u}}\} = 0, \tag{3}$$

where **K** and **M** represent the global stiffness and mass matrices, respectively. The mass and stiffness matrices are represented as symmetric $2n \times 2n$ matrices when modelling a two-dimensional truss structure and $3n \times 3n$ matrices for a three-dimensional truss structure. The size of these global matrices will be reduced by the number of supported degrees of freedom, since there are no displacements at these locations. Given that the displacement vector is harmonic, (3) may be restructured into the generalized eigenvalue problem:

$$\mathbf{K}\boldsymbol{\phi}_j = \lambda_j(\mathbf{M} + \mathbf{M}_0)\boldsymbol{\phi}_j, \tag{4}$$

where **M** refers to the global mass matrix for the structure's bar elements, $\mathbf{M}_0$ refers to the additional mass of the nodes connecting each element and $\lambda_j$ represents the eigenvalue for a given mode of vibration $\boldsymbol{\phi}_j$ ($j = 1, 2, 3, \ldots$). The free vibrations of a structure are equal to the square root of the eigenvalues $\omega_j^2 = \lambda_j$ in radians per second, and thus the natural frequencies and normal modes of vibration for the structure may be determined.

### 2.3. Frequency formulation

#### 2.3.1. Determine the reference frequencies

To determine conformance with the original design problem, it is necessary to calculate the natural frequencies of the structure. If a candidate design has been obtained via layout optimization, then this can be performed using the connectivity and member cross-sectional areas generated in the optimization. The areas for each element are multiplied by the corresponding mass and stiffness coefficients before being assembled into the global matrices (**K** and **M**) at the row/column index corresponding to the degrees of freedom associated with the member end nodes, with rows and columns related to the supported degrees of freedom omitted. The eigenvalues can be extracted *e.g.* using the built-in MATLAB® `eigs` functionality. Previous studies, *e.g.* Du and Olhoff (2007), have considered multiple eigenfrequencies; however, this contribution will concentrate on just the first natural frequency in hertz for the structure to ensure it will not resonate when exposed to a source of excitation.

#### 2.3.2. Semidefinite constraint

In order to perform an optimization targeting the natural frequencies of the structure, a new constraint equation must be derived from the generalized eigenvalue problem (4). Once the coefficient matrices for stiffness and mass are determined, in order to avoid the optimization generating a structure prone to low frequency vibration, a threshold can be set such that the smallest eigenvalue from (4)

is greater than or equal to a defined minimum value. Thus (4) may be transformed into the following constraint:

$$\mathbf{K}(\boldsymbol{a}) - \lambda(\mathbf{M}(\boldsymbol{a}) + \mathbf{M}_0) \succcurlyeq 0, \tag{5}$$

where $\mathbf{K}(\boldsymbol{a}) = \sum_{i=1}^{m} a_i \mathbf{K}_i$ and $\mathbf{M}(\boldsymbol{a}) = \sum_{i=1}^{m} a_i \mathbf{M}_i$ are the global stiffness and mass matrices, respectively, $a_i$ refers to the cross-sectional area of member $i$, $\lambda$ is the eigenvalue derived from the minimum specified natural frequency ($\omega_1$) for the specified mode of vibration $\boldsymbol{\phi}_j$ and $\succcurlyeq$ indicates that the matrix to its left is symmetric and positive semidefinite. For the purposes of this contribution, the connecting nodes are not considered and therefore the mass associated with joints $\mathbf{M}_0 = 0$.

Thus, when incorporated into the layout optimization formulation (1), the problem may be written as

$$\begin{aligned} \min_{\boldsymbol{a},\boldsymbol{q}} \quad & V = \mathbf{l}^{\mathrm{T}}\boldsymbol{a} \\ \text{s.t.} \quad & \begin{cases} \mathbf{B}\boldsymbol{q} = \mathbf{p}, & \\ \mathbf{K}(\boldsymbol{a}) - \lambda_0 \mathbf{M}(\boldsymbol{a}) \succcurlyeq 0 & \\ -\sigma^{-} a_i \le q_i \le \sigma^{+} a_i, & \forall\, i \\ a_i \ge 0, & \forall\, i. \end{cases} \end{aligned} \tag{6}$$

Fixing the smallest eigenvalue ($\lambda_0$) to be greater than or equal to the minimum specified frequency ensures that the areas of the elements are adjusted as part of the optimization until the inequality constraint is achieved. Incorporation of the semidefinite constraint means that an SDP solver is now required to solve the problem. Note that SDP problems are convex, enabling a globally optimal solution to be obtained, but are considerably more computationally demanding to solve than their LP counterparts.

### 2.4. Short cantilever example

Two means of optimizing a short cantilever structure based on a prescribed minimum first natural frequency will now be outlined, using the example problem defined in Figure 2 to illustrate salient points. For this problem: $P = 1 \times 10^3$ N; $E = 210 \times 10^9$ N m$^{-2}$; $\rho = 8050$ kg m$^{-3}$; and the limiting tensile and compressive stresses $\sigma = 350 \times 10^6$ Pa. The prescribed constraint on the fundamental natural frequency is $f_1 \ge 425$ Hz. All numerical examples in this contribution were run on a 64 bit Windows® 10 desktop PC equipped with an Intel® i5 3.7 GHz processor and 32 GB of RAM, using a script programmed using MATLAB 2020b. A number of semidefinite solvers are available and are compared by Tyburec and Zeman (2017). This contribution will initially employ the MOSEK ApS (2017) v8.1 solver using the Java Fusion MATLAB interface. It should be noted that unless otherwise specified all layouts presented in the figures are filtered to include only elements with areas greater than $1 \times 10^{-6}$ m$^2$. This may occasionally result in elements that appear to be disconnected from the overall structure. Additionally, to facilitate comparison with other published work, non-dimensional volumes $V$ are presented throughout the article, with scaled volumes $V(P/\sigma)$ in cubic metres also included in accompanying tables for completeness.

#### 2.4.1. Two phase optimization approach

Since SDP problems are computationally expensive to solve, initially the efficacy of a two phase optimization approach is evaluated. With this approach, a traditional layout optimization is first undertaken without considering frequency constraints; if prescribed frequency requirements are not met by the generated design, then a size optimization is subsequently performed to ensure that these are met, modifying only the subset of elements present in the optimal structure; *i.e.* in this second phase the areas of each element $a_i$ are adjusted to ensure the semidefinite constraint (5) is met. In the interests of computational efficiency, only those elements that have an area greater than a predetermined minimum (taken as $1 \times 10^{-6}$ m$^2$) are included in the optimization; these elements will henceforth be referred to as members.

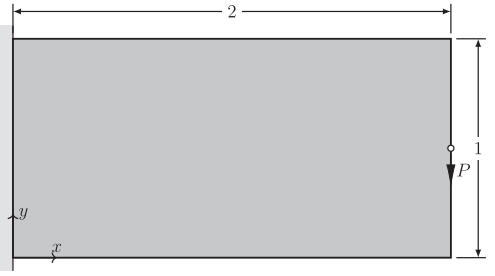


**Figure 2.** Short cantilever example: design domain, loading and support details. All dimensions are in metres.

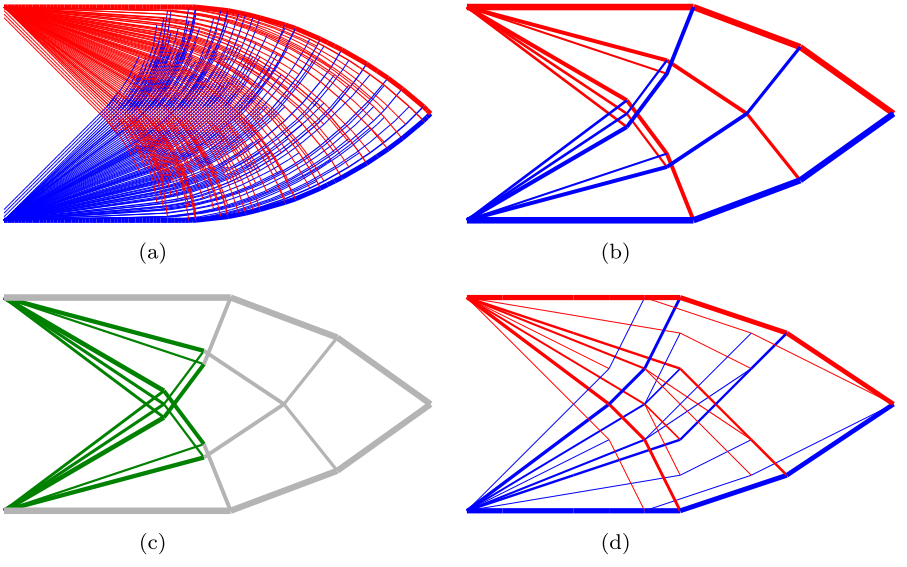


**Figure 3.** Short cantilever example: (a) reference LP solution achieved using layout optimization using 120 × 60 nodal divisions; (b) more practical LP layout, achieved by reducing the nodal divisions to 40 × 20 and penalising joints; (c) outcome of the SDP frequency optimization performed on the practical layout from (b); (d) layout generated using SDP optimization of the full ground structure, including frequency constraint using 12 × 6 nodal divisions. (Key: red = tension; blue = compression; green = members in (c) whose areas have been modified compared with (b); grey = members whose areas are as per the layout in (b) [online only]. (For (a) $V = 7.030$, $f_1 = 403$ Hz. (b) $V = 7.095$, $f_1 = 410$ Hz. (c) $V = 7.436$, $f_1 = 425$ Hz and (d) $V = 7.134$, $f_1 = 425$ Hz.)

**Table 1.** Short cantilever example: LP and SDP results (target frequency for the SDP problem = 425 Hz).

| Figure | Model | Nodal divisions | $V$ | $V(P/\sigma)$ ($\times 10^{-5}$m$^3$) | $f_1$ (Hz) | Time (s) |
|---|---|---|---|---|---|---|
| 3(a) | LP (fine ref.) | 120 × 60 | 7.030 | 2.009 | 403 | 146 |
| 3(b) | LP | 40 × 20 | 7.095 | 2.027 | 410 | 26 |
| 3(c) | SDP (size only) | … | 7.436 | 2.125 | 425 | 3 |
| … | LP (coarse ref.) | 12 × 6 | 7.116 | 2.033 | 407 | 9 |
| 3(d) | SDP (full) | 12 × 6 | 7.134 | 2.038 | 425 | 1472 |

Considering first the example problem defined in Figure 2, an initial layout optimization is carried out to provide reference values for the volume and first natural frequency of the structure; see Table 1 and Figure 3(a). The structure shown is similar to that obtained by He, Gilbert, and Song (2019).

However, the reference structure contains many members, so for the first phase of the proposed two phase procedure a domain with fewer nodes is used to enable a more practical layout to be generated, containing fewer 'fibrous' elements. This is achieved by both reducing the number of nodes and

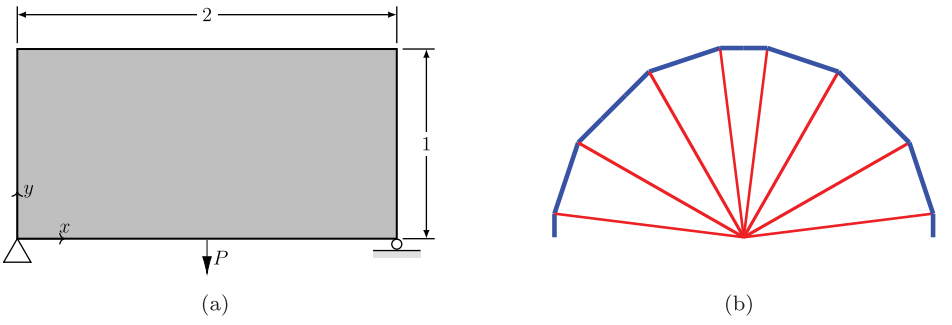


**Figure 4.** Half wheel example: (a) problem definition; (b) optimal structure obtained after phase one of the two phase method (*i.e.* not considering frequency constraints). All dimensions are in metres.

introducing a joint penalty, after Parkes (1975). This results in the structure shown in Figure 3(b), which has fewer joints and elements than the benchmark but which has a similar volume.

In the second phase, the structure from the first phase is re-optimized using the modified formulation that includes frequency constraints (6) to revise member sizes ensuring the frequency is not less than 425 Hz. In the re-optimization it is found that the areas of diagonal members radiating from the support line, along with some members interconnecting these, need to be modified (resized members are highlighted in green in Figure 3(c) in the online version of the paper).

It is evident that the solver has been successful in achieving the desired minimum natural frequency, at minimal CPU cost; however, this has in this case come at a relatively high cost in terms of increased volume (8.7%). This suggests that changing the size of the elements alone may not lead to the most efficient solution, and a better one may be available if a wider solution space were to be made available.

Next consider the classical half-wheel problem shown in Figure 4, as originally studied by Michell (1904). The problem involves a central point load $P = 1 \times 10^3$ N applied at midspan between statically determinate supports, limiting tensile and compressive stresses $\sigma = 350 \times 10^6$ Pa and, in common with the other presented examples, $E = 210 \times 10^9\,\mathrm{N\,m^{-2}}$ and $\rho = 8050\,\mathrm{kg\,m^{-3}}$. The optimal solution obtained when using $16 \times 8$ nodal divisions is shown in Figure 4(b) and has a non-dimensional volume $V = 3.191$. This includes a short vertical member above each of the supports, leading to a structure that is in unstable equilibrium with the applied loading. This arises because only equilibrium (and strength) constraints are enforced in phase one. However, a byproduct of this is that subsequently adjusting the sizes of structural members alone in the second phase, with a view to achieving a natural frequency of for example $f_1 = 200$ Hz, will fail owing to inherent instability in the problem. This highlights a further limitation of the two phase optimization approach.

### 2.4.2. Holistic optimization

Although the two phase approach described in the preceding section is computationally efficient for problems where it can obtain viable solutions, if the increase in volume in the second phase is large then the question arises as to whether a more materially efficient design exists.

This can be checked by applying the formulation including an SDP frequency constraint to the full ground structure. The associated computational expense means that only a coarse nodal grid ($12 \times 6$) can be used in this case. For the short cantilever example, the solution obtained using the finest nodal density achievable with the available memory is shown in Figure 3(d). When compared with a reference structure consisting of the same size, it demonstrates that a modified design enables the target frequency to be met with little impact on the overall volume of the structure. The optimum point where the equilibrium and frequency constraints are satisfied requires a layout different from that of the structural optimization alone. However, it must be noted that the largest problem that could be solved with a fully connected ground structure is much smaller than the one that could be solved using the two phase approach.

## 3. SDP formulation with member adding

To solve complex problems of this nature with a large initial ground structure efficiently, a special purpose solver based on the Mehrota-type primal–dual interior point method (Fujisawa *et al.* 2000) was developed. The approach and its implementation closely follow Weldeyesus *et al.* (2019), which describes the optimization of truss structures with constraints on global stability modelled via SDP. In Weldeyesus *et al.* (2019), the proposed method is capable of obtaining solutions to relatively large problems that could not otherwise have been solved. Owing to similarities between the mathematical properties of the optimization problem considered in this article and those of the problem discussed in Weldeyesus *et al.* (2019), only the member adding method is explained here in detail. Issues such as exploiting sparsity and the low rank property of the element stiffness matrices $\mathbf{K}_i$ and mass matrices $\mathbf{M}_i$ when forming the linear systems arising in the interior point algorithm for SDP are not repeated here, but play a crucial role in the overall efficiency of the approach. As outlined in Section 2.1, the adaptive member adding approach—which is based on the column generation technique, see Gondzio and Sarkissian (1996), Desrosiers and Lübbecke (2005) and Gondzio, González-Brevis, and Munari (2013)—is an iterative process originally proposed in Gilbert and Tyas (2003), and also applied to other problems by *e.g.* Sokół and Rozvany (2013) and Weldeyesus and Gondzio (2018), who also employed linear programming to obtain solutions. The method was extended to treat SDP problems by Weldeyesus *et al.* (2019). The procedure starts by solving a minimum connectivity ground structure problem (Figure 1(d)), and proceeds by adding elements from a potential connection list until a solution that satisfies the original fully connected ground structure problem is obtained. This approach enables the method to obtain a solution using a small fraction of the large number of potential connections: see Gilbert and Tyas (2003) and Weldeyesus *et al.* (2019) for supporting numerical results.

### 3.1. Details of the SDP member adding algorithm

Here, a mathematical description of the member adding procedure akin to that described in Section 4 of Weldeyesus *et al.* (2019) is presented. The primal problem (6) has an associated dual problem (7), where $\boldsymbol{u} \in \mathbb{R}^n$ and $\boldsymbol{X} \in \mathbb{S}^n_+$ (*i.e.* $\boldsymbol{X}$ is symmetric and positive semidefinite) are the Lagrange multipliers for the equilibrium equation and the matrix inequality constraints in (6), respectively. Note that, in some literature, for example Wolkowicz, Saigal, and Vandenberghe (2000), the primal formulation (6) is stated as dual and the dual problem formulation (7) as primal.

$$\begin{aligned} \underset{\boldsymbol{u},\boldsymbol{X}}{\text{maximize}} \quad & \mathbf{p}^{\mathrm{T}}\boldsymbol{u} \\ \text{subject to} \quad & -\frac{1}{\sigma^-}(l_i - (\mathbf{K}_i - \lambda\mathbf{M}_i) \bullet \boldsymbol{X}) \le (\mathbf{B}^{\mathrm{T}}\boldsymbol{u})_i, \quad \forall\, i \\ & (\mathbf{B}^{\mathrm{T}}\boldsymbol{u})_i \le \frac{1}{\sigma^+}(l_i - (\mathbf{K}_i - \lambda\mathbf{M}_i) \bullet \boldsymbol{X}), \quad \forall\, i \\ & \boldsymbol{X} \succeq 0. \end{aligned} \tag{7}$$

After solving, the dual violations can be obtained using only the variables $\boldsymbol{u}$ and $\boldsymbol{X}$ in (7). The process is as follows.

For any variable corresponding to member $i$ to be dual feasible, formulation (7) implies that the relation

$$-\frac{1}{\sigma^-} \le \frac{1}{l_i - (\mathbf{K}_i - \lambda\mathbf{M}_i) \bullet \boldsymbol{X}}(\mathbf{B}^{\mathrm{T}}\boldsymbol{u})_i \le \frac{1}{\sigma^+} \tag{8}$$

is satisfied. Now suppose that $I_0 \subset \{1, \ldots, m\}$ is a set of indices of members for which the primal problem (6) and its dual (7) are currently solved. After solving problem (6), and obtaining dual

**Table 2.** Short cantilever example: fully connected ground structure and member adding approaches (target frequency = 425 Hz).

| Figure | Model | Nodal divisions | $V$ | $V(P/\sigma)$ ($\times 10^{-5}$ m$^3$) | Time (s) | Speed up | Memory (MB) |
|---|---|---|---|---|---|---|---|
| 3(d) | SDP (full) | 12 × 6 | 7.134 | 2.038 | 1,472 | … | 16,081 |
| 5(a) | SDP (mem. add.) | 12 × 6 | 7.134 | 2.038 | 8 | ×183 | 5 |

**Table 3.** Short cantilever example: results from the SDP member adding algorithm.

| Figure | Nodal divisions | $V$ | $\Delta V$[a] (%) | $V(P/\sigma)$ ($\times 10^{-5}$m$^3$) | $f_1$ (Hz) | Time (s) |
|---|---|---|---|---|---|---|
| 5(b) | 40 × 20 | 7.064 | +0.5 | 2.018 | 425 | 4,915 |
| 5(c) | 40 × 20 | 7.129 | +1.4 | 2.037 | 450 | 11,655 |
| 5(d) | 40 × 20 | 7.597 | +8.0 | 2.171 | 480 | 17,671 |

[a]Percentage change compared with the volume of the reference structure shown in Figure 3(a).

values corresponding to (7), for all members with indices in $I_0$, condition (8) can be used for all $i \in \{1, \ldots, m_0\} \backslash I_0$ to generate a set $I$ of member indices to be added, given by

$$I = \left\{ i \in \{1, \ldots, m_0\} \backslash I_0 \,\middle|\, \frac{1}{l_i - (\mathbf{K}_i - \lambda \mathbf{M}_i) \bullet \boldsymbol{X}^*} (\sigma^- \varepsilon_i^- + \sigma^+ \varepsilon_i^+) \geq 1 + \beta \right\}, \tag{9}$$

where the virtual strains are $\varepsilon_i^+ = \max\{(\mathbf{B}^{\mathrm{T}} \boldsymbol{u}^*)_i, 0\}$ and $\varepsilon_i^- = \max\{-(\mathbf{B}^{\mathrm{T}} \boldsymbol{u}^*)_i, 0\}$ with $\boldsymbol{u}^*$ and $\boldsymbol{X}^*$ being optimal points of the preceding subprogram and $\beta > 0$ is an allowed tolerance decided by the user. If $I = \emptyset$ the member adding procedure terminates; otherwise, members with indices in $I$ are added to the subsequent problem, filtering these using the heuristic techniques described in Weldeyesus and Gondzio (2018) if necessary to avoid problem size growing too rapidly.

### 3.2. Revisiting the short cantilever and half-wheel examples

In order to establish the gains in efficiency from utilising the new member adding-based SDP algorithm, the problem given in Figure 2 will be revisited, initially replicating the problem in Figure 3(d) to demonstrate the efficiency gains of using the member adding algorithm.

Results for coarse nodal grids are presented in Table 2 and Figure 5(a). It is evident that the optimal volumes are identical irrespective of whether a fully connected ground structure or member adding is employed, and the optimal truss solutions shown in Figures 3(d) and 5(a) are also virtually identical. Most significantly, it is also evident that the proposed member adding algorithm can obtain a solution over two orders of magnitude more quickly than when a fully connected ground structure is used, with the memory requirements reduced by three orders of magnitude. These efficiency improvements mean that problems involving relatively fine nodal grids can now be tackled, which was not possible before. Thus, revisiting the problem shown in Figure 3(a), a new solution obtained via member adding is presented in Figure 5(b), with additional solutions presented for higher minimum target frequencies in Figures 5(c) and 5(d). Corresponding computational details are shown in Table 3. This shows that relatively fine grid problems can be tackled, and that the geometry of the optimal structure changes when higher target frequencies are specified, with the overall volume also increasing.

Now revisiting the half wheel example, by applying the procedure proposed in this contribution a structure that satisfies both equilibrium and frequency constraints can be generated. For a target frequency of 200 Hz, the generated solution is negligibly higher in non-dimensional volume (now $V = 3.193$, just 0.05% greater than before); see Figure 6. Significantly, to satisfy the frequency constraint, it is evident that additional stabilizing members have been added—although in this case some of these are very thin, with some radial members below the filter cut-off (in this case area = $6 \times 10^{-8}$m$^2$) omitted.

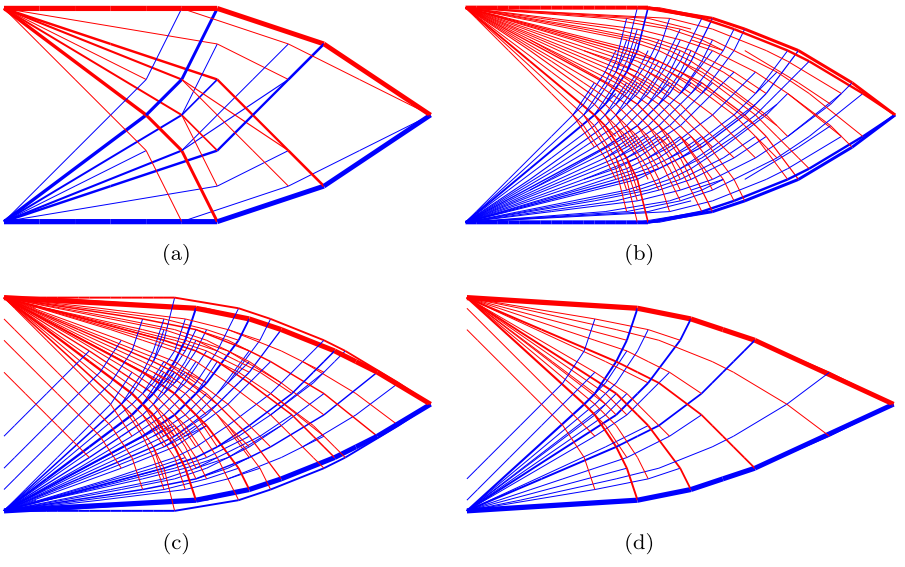


**Figure 5.** Short cantilever example: results obtained using the SDP member adding method for a range of minimum frequencies. A total of 12 × 6 nodal divisions are used in case (a) and 40 × 20 in cases (b)–(d). (For (a) $V = 7.134, f_1 = 425$ Hz. (b) $V = 7.064, f_1 = 425$ Hz. (c) $V = 7.129, f_1 = 450$ Hz and (d) $V = 7.597, f_1 = 480$ Hz.)

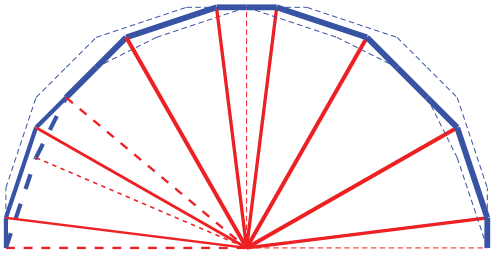

**Figure 6.** Half wheel example: structure obtained using combined equilibrium and frequency constraints for a target frequency of 200 Hz (dashed lines indicate members added to satisfy the frequency constraint, also helping to stabilize the structure).

### 3.3. *Influence of initial member arrangement on computation*

It has been demonstrated that the inclusion of a member adding step in the optimization reduces the memory burden and enables problems of significant size to be tackled. To understand the performance of the member adding method further, the examples originally considered by Gilbert and Tyas (2003) are used to investigate the influence of the chosen initial nodal connectivity on the solution, the computational time and the required memory footprint. A 28 × 28 nodal division square domain is used; however, in this contribution overlapping connections are omitted as they can lead to instability in the frequency calculations due to multiple members coexisting in the same space. In addition, due to the significant memory requirements of the fully connected ground structure example (circa 400 GB), an additional set of results is obtained using a domain comprising a reduced number of 14 × 14 nodal divisions.

Applying the same physical parameters as in the example shown in Figure 2, the original optimal truss structure from Gilbert and Tyas (2003) was assessed and found to have a first natural frequency of $f_1 = 945$ Hz; therefore, an initial frequency target of $f_1 = 950$ Hz was considered appropriate for the starting problem as it is close to the original yet includes an active frequency constraint. The

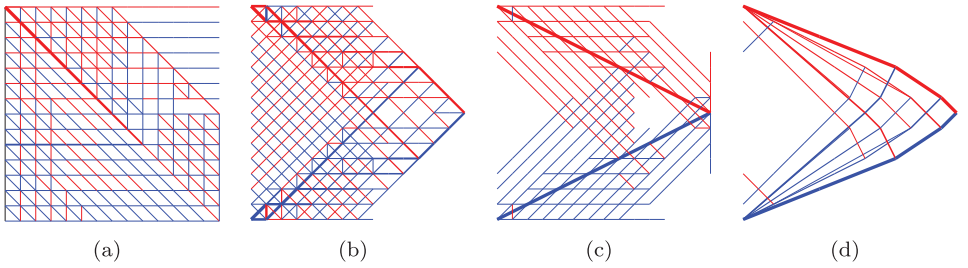


**Figure 7.** Influence of initial connectivity in member adding scheme: (a) adjacent nodes connected (right to left upward diagonals in all units), iteration 1; (b) minimally connected ground structure with nearest neighbour nodes connected, iteration 1; (c) minimally connected ground structure plus boundary/loaded nodes connected, iteration 1; (d) final optimized structural form common to all starting points.

target frequency was then increased by 10% to help verify the extent to which the influence of the initial member connectivity is common across a range of target frequencies.

Table 4 shows the four initial ground structures considered, (a)–(d), together with results for the two target frequencies for each of the two nodal division discretizations; note that, to maintain a basis for comparison, all presented volumes are non-dimensional. The resulting volumes for all the cases are within 1% of those provided in the original article, demonstrating that in this case the frequency constraint does not come at a high cost in terms of structural efficiency; however, CPU times are markedly increased. In contrast to the findings in the original article by Gilbert and Tyas (2003), here it is also clear that the most efficient initial ground structure in terms of CPU time comprises a ground structure with the supports directly connected to the load (case (c)); in addition, this leads to a lower number of peak LP variables, indicating a reduced memory burden. Figure 7 shows the outcome of the initial iteration for each of the three initial ground structures investigated when using the member adding scheme for the $14\times14$ nodal division case. It is evident that, although the supports are in each case connected to the load, in the case of (c) this is predominantly achieved through the use of just two diagonal elements, which directly connect the load with the supports.

It should be noted that, when member adding is used, ground structure (a) has the longest associated CPU time, and also the greatest number of LP variables at the end of the optimization process. Ground structure (c) has the shortest associated CPU time, the fewest LP variables, and hence also the lowest memory consumption. However, for the sake of simplicity, initial ground structure (b) will be used for all subsequent examples in this contribution. Finally, it should also be noted that, although the optimized volume obtained when using a fully connected ground structure from the outset, (d), is marginally higher than that obtained in the other three cases, this is probably due to the contribution to the volume of a large number of elements with areas very close to zero.

## 4. Numerical examples

A wider range of examples are now considered to investigate the efficacy of the presented SDP member adding algorithm further when used to optimize a component, considering simultaneously equilibrium, strength and first natural frequency constraints. The classical Hemp cantilever and MBB beam examples are first considered. A 3D cantilever designed to carry a point load is then considered, with different minimum specified natural frequencies used to show the resulting variation in form and associated volume. Each example begins with a minimum connectivity ground structure.

### *4.1. Hemp cantilever example*

The initial example considered was first studied by Hemp (1973) and consists of a square domain with single point load located at mid-height between two supports, as shown in Figure 8(a).

**Table 4.** Influence of initial member connectivity on efficiency of member adding scheme: (a) adjacent nodes connected (right to left upward diagonals in all cells); (b) minimally connected ground structure, comprising nearest neighbour connectivity; (c) minimally connected ground structure plus connections between boundary and loaded nodes; (d) traditional fully connected ground structure (without overlapping bars).

| Grid | $f_1$ (Hz) | | (a) | (b) | (c) | (d) |
|---|---|---|---|---|---|---|
| 28 × 28 | 950 | Volume, $V$ | 2.432 | 2.432 | 2.432 | – |
| | | No. of iterations | 9 | 6 | 7 | – |
| | | Initial no. of bars | 2,408 | 3,192 | 3,221 | – |
| | | Peak no. of bars | 36,151 | 8,000 | 5,881 | – |
| | | Time to 1.001$V$ (s) | 63,875.1 | 2,209.9 | 804 | – |
| | | CPU time (s) | 182,738.9 | 3,811.6 | 2,102.8 | – |
| | 1,045 | Volume, $V$ | 2.441 | 2.441 | 2.441 | – |
| | | No. of iterations | 12 | 7 | 8 | – |
| | | Initial no. of bars | 2,408 | 3,192 | 3,221 | – |
| | | Peak no. of bars | 33,964 | 10,710 | 7,005 | – |
| | | Time to 1.001$V$ (s) | 192,161.2 | 4,054.9 | 992 | – |
| | | CPU time (s) | 289,679.8 | 8,555.2 | 2,852.6 | – |
| 14 × 14 | 950 | Volume, $V$ | 2.435 | 2.435 | 2.435 | 2.437 |
| | | No. of iterations | 9 | 6 | 6 | – |
| | | Initial no. of bars | 616 | 812 | 827 | 15,556 |
| | | Peak no. of bars | 4,239 | 1,982 | 1,197 | 15,556 |
| | | Time to 1.001$V$ (s) | 660.2 | 69.9 | 29.1 | – |
| | | CPU time (s) | 1,379.1 | 116.7 | 51.2 | 5,501.3 |
| | 1,045 | Volume, $V$ | 2.443 | 2.443 | 2.443 | 2.448 |
| | | No. of iterations | 9 | 6 | 5 | – |
| | | Initial no. of bars | 616 | 812 | 827 | 15,556 |
| | | Peak no. of bars | 3,365 | 1,936 | 1,265 | 15,556 |
| | | Time to 1.001$V$ (s) | 346 | 67.4 | 33.8 | – |
| | | CPU time (s) | 748.1 | 134.8 | 45.5 | 5,089.7 |

**Table 5.** Hemp cantilever example: results obtained from equilibrium optimization and with inclusion of the frequency constraints.

| Figure | Model | Nodal divisions | $V$ | $\Delta V$ (%) | $V(P/\sigma)$ ($\times 10^{-5}$m$^3$) | $f_1$ (Hz) | Time (s) |
|---|---|---|---|---|---|---|---|
| 8(b) | REF | 72 × 72 | 4.332 | … | 1.238 | 616 | 194 |
| … | LP | 48 × 48 | 4.339 | +0.01 | 1.240 | 623 | 17 |
| 8(c) | SDP | 48 × 48 | 4.340 | +0.01 | 1.240 | 700 | 42,676 |
| 8(d) | SDP | 48 × 48 | 4.794 | +10.6 | 1.370 | 1,000 | 75,004 |

Hemp determined the non-dimensional analytical volume to be approximately 4.34; later, He and Gilbert (2015) applied more precise methods and geometry rationalization, further reducing the optimum volume to 4.3228. Here, a nodal grid comprising 72 × 72 nodal divisions and the material properties $P = 1 \times 10^3$ N, $E = 210 \times 10^9$ N m$^{-2}$, $\rho = 8050$ kg m$^{-3}$ and the limiting tensile and compressive stresses $\sigma = 350 \times 10^6$ Pa were used to obtain a reference LP solution with a volume $V = 4.332$, within 0.5% of the improved optimum figure. The associated structure is shown in Figure 8(b). The first natural frequency of this reference structure was computed to be $f_1 = 616$ Hz.

In order to generate solutions in a reasonable timescale for the SDP analyses, the nodal density was reduced to 48 × 48. An additional LP reference was obtained at this density that has negligible impact on volume but changes the first frequency to 686 Hz. SDP analyses were conducted with target first natural frequencies of $f_1 = 700$ and 1000 Hz to identify changes in the generated structure. Results of the associated optimization runs are presented in Table 5 and Figures 8(c) and 8(d), respectively.

In the first case, the impact on the resulting generated structure and associated volume is small, with the increase in volume being less than 1% and little difference in overall layout. In the second case,

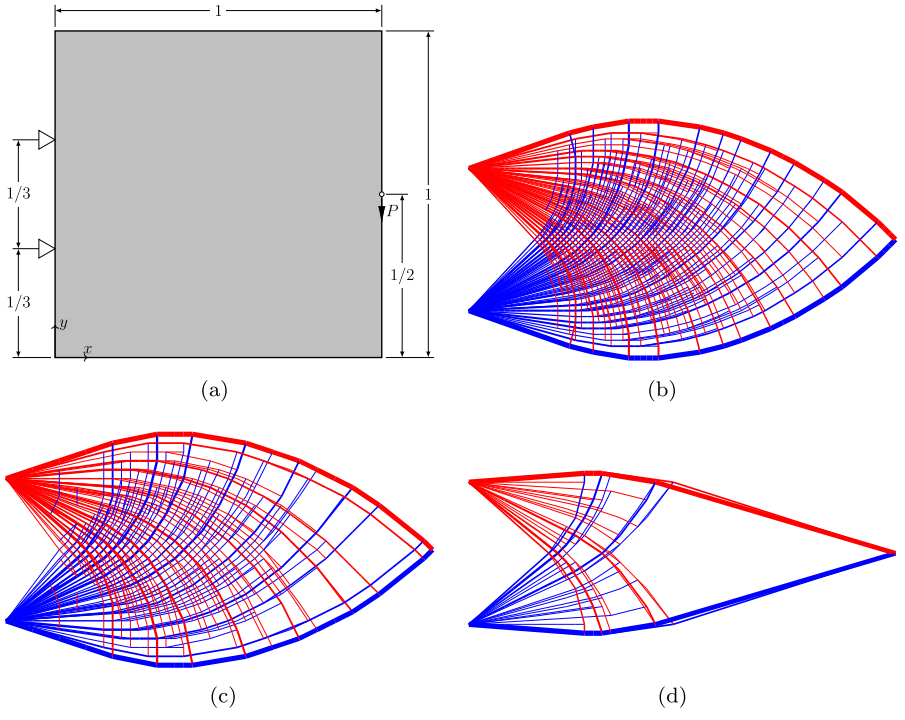


**Figure 8.** Hemp cantilever example: (a) problem definition with dimensions in metres; (b) reference LP solution, obtained with 72 × 72 nodal divisions; (c) SDP member adding solution obtained for a target frequency of 700 Hz; (d) SDP member adding solution obtained for a target frequency of 1000 Hz. Note that both (c) and (d) have 48 × 48 nodal divisions. (For (b) $V = 4.332$, $f_1 = 616$ Hz. (c) $V = 4.350$, $f_1 = 700$ Hz and (d) $V = 4.794$, $f_1 = 1000$ Hz.)

increasing the minimum frequency to $f_1 = 1000$ Hz can be observed to have a much more significant impact, with the overall structural depth and complexity of the result both reduced.

### 4.2. MBB beam example

The Messerschmidt–Bölkow–Blohm (MBB) beam is attributed to the German aircraft company of the same name, and can still be found in Airbus passenger aircraft. Though the real-world problem includes a number of design constraints, in the literature a simpler problem is normally considered, involving simple loading and boundary conditions and usually targeting minimum volume or compliance. The exact analytical layout for the MBB structure with stress constraints was derived by Rozvany (1998), with the optimal non-dimensional volume $V = 13.597$ for a beam length of three. As the beam is symmetrical, only the right half is shown in Figure 9(a). An optimization was carried out with nodes directly along the symmetry plane free to move vertically whilst the bottom right corner was fixed in the vertical direction and free to move horizontally. The example assumes aerospace grade aluminium is used with $P = 1 \times 10^3$ N, $\sigma = 90 \times 10^6$ Pa, $E = 68.9 \times 10^9$ N m$^{-2}$ and $\rho = 2770$ kg m$^{-3}$.

An initial LP optimization was carried out to obtain a reference volume and frequency for the structure, using 60 × 20 nodal divisions to provide a balance between accuracy and computational efficiency (Figure 9(b)). SDP solutions were then sought for two minimum target frequencies; the solutions obtained (Table 6 and Figures 9(c) and 9(d)) demonstrate that the introduction of a frequency constraint has enabled minimum volume structures satisfying a given minimum frequency to be obtained, with very little impact on overall volume. However, it is evident that the time required

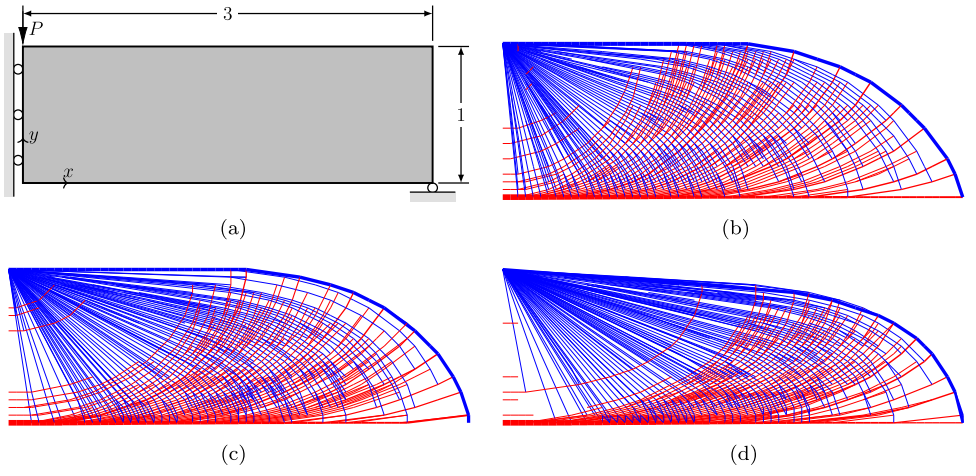


**Figure 9.** MBB beam example: (a) problem definition with dimensions in metres; (b) reference solution obtained for this example with the determined first natural frequency; (c) SDP member adding solution obtained for a target frequency of 400 Hz; (d) a target of 425 Hz. (For (b) $V = 14.136, f_1 = 374$ Hz. (c) $V = 14.237, f_1 = 400$ Hz and (d) $V = 14.631, f_1 = 425$ Hz.)

**Table 6.** MBB beam example: SDP member adding algorithm results.

| Figure | Model | Nodal divisions | $V$ | $\Delta V$ (%) | $V(P/\sigma)$ ($\times 10^{-4}$m$^3$) | $f_1$ (Hz) | Time (s) |
|---|---|---|---|---|---|---|---|
| 9(b) | LP | 60 × 20 | 14.136 | … | 1.571 | 374 | 8 |
| 9(c) | SDP | 60 × 20 | 14.238 | +0.72 | 1.582 | 400 | 31,781 |
| 9(d) | SDP | 60 × 20 | 14.631 | +3.5 | 1.626 | 425 | 46,317 |

to complete a frequency optimization is clearly considerably longer than that required for a basic LP optimization.

### 4.3. 3D cantilever example

The third example is a simple 3D cantilever beam, as shown in Figure 10(a). To improve the clarity of the results and to minimize the additional computational burden associated with solving 3D problems, the number of nodal divisions has been reduced to $6 \times 2 \times 2$ to ensure solutions are obtained in a manageable time-frame. The properties for this example are as follows: $P = 1 \times 10^3$ N; $E = 210 \times 10^9$ N m$^{-2}$; $\rho = 8050$ kg m$^{-3}$; and the maximum tensile and compressive stresses are $\sigma = 350 \times 10^6$ Pa. Various target first natural frequencies are used to demonstrate the change in structural form that results from including a frequency constraint.

Full results for this example are shown in Table 7. Figure 10(b) shows the layout of the optimal structure based solely upon equilibrium and strength considerations, with the natural frequency of the resulting structure being found to be 57 Hz. When a frequency constraint $f_1 = 100$ Hz is introduced (Figure 10(c)) the structure begins to change, with new members added to the structure. Similar to the 2D examples, these additional elements brace the structure, adding stiffness and therefore increasing the frequency; however, the use of member adding has allowed this to happen in a short amount of time and with limited impact on the overall volume of the structure. As the target frequency is increased further to 150 and 200 Hz as shown in Figures 10(d) and 10(e), respectively, a more dramatic change begins to take place, with the members that are primarily taking the load and providing structural stiffness becoming longer and growing in cross section.

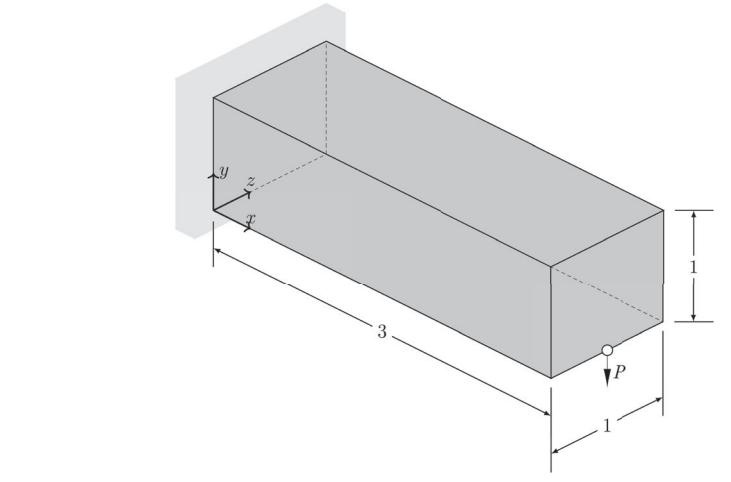


(a)

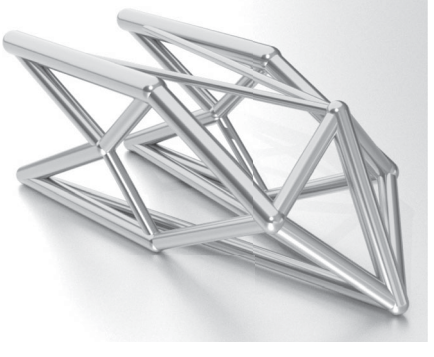

(b)

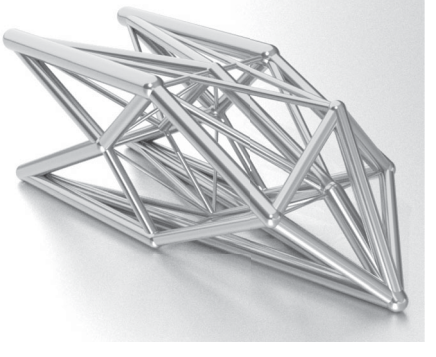

(c)

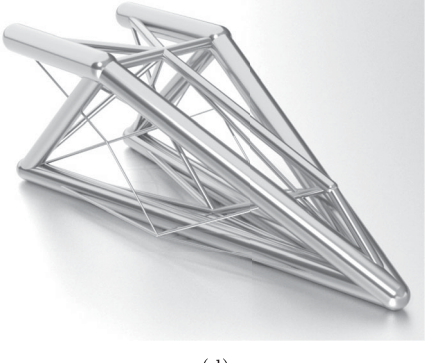

(d)

(e)

**Figure 10.** 3D cantilever example: (a) problem definition with dimensions in metres; (b) LP solution (no frequency constraint); (c) SDP member adding solution for a target frequency of 100 Hz; (d) target of 150 Hz; (e) target of 200 Hz. All cases employ $6 \times 2 \times 2$ nodal divisions. (For (b) $V = 30.676, f_1 = 57$ Hz. (c) $V = 30.883, f_1 = 100$ Hz. (d) $V = 33.233, f_1 = 150$ Hz and (e) $V = 38.111, f_1 = 200$ Hz.)

**Table 7.** 3D cantilever example: SDP member adding algorithm results.

| Figure | Model | Cons | $V$ | $\Delta V$ (%) | $V(P/\sigma)$ ($\times 10^{-5} m^3$) | $f_1$ (Hz) | Time (s) |
|---|---|---|---|---|---|---|---|
| 10(b) | LP | 474 | 30.676 | … | 8.765 | 57 | 5.8 |
| 10(c) | SDP | 566 | 30.883 | +0.6 | 8.824 | 100 | 9.9 |
| 10(d) | SDP | 633 | 33.233 | +8.3 | 9.495 | 150 | 12.6 |
| 10(e) | SDP | 582 | 38.111 | +24.2 | 10.889 | 200 | 13.3 |

## 5. Conclusions

Numerical layout optimization provides an efficient means of generating optimal truss structures for a given set of design requirements. However, traditional linear programming-based formulations are limited, and cannot for example accommodate frequency constraints. In this contribution, extended semi-definite programming-based formulations are considered that allow the minimum first natural frequency of a structure to be specified. The main conclusions are as follows.

- The use of a two phase approach, in which the traditional LP layout optimization formulation is used in the first phase and an SDP size optimization is used in the second phase, provides a computationally efficient means of generating solutions satisfying a specified frequency constraint. However, the solutions obtained are likely to be sub-optimal, with the resulting structures having higher than necessary volume.
- Alternatively, a constraint on frequency can be introduced in the optimization directly, furnishing layouts that satisfy both structural performance and first natural frequency requirements. However, when using a fully connected ground structure and a standard SDP solver, the computational cost and memory requirements have been found to be high, severely limiting the scale of problem that can be tackled.
- The use of a bespoke solver and an adaptive member adding solution strategy, which involves starting with a sparsely connected ground structure and only adding members as required until the optimal solution is found, allows solutions to be obtained in a much shorter time-frame (183 times quicker in the case of one of the examples considered), and with much lower memory consumption. This approach has been successfully applied to a range of 2D and 3D problems in this article.

In future studies, the influence of joints on vibration characteristics will be considered in more detail, with for example differences in optimal layout and volume being evaluated when rigid-joints as opposed to pin-joints are assumed. In addition, consideration will be given to limiting the number and arrangement of members within a final design, to ensure the resulting component is readily manufacturable.

## Acknowledgments

The assistance of Dr Linwei He in producing the graphics for Figures 10(b)–10(e) is gratefully acknowledged.

## Data availability statement

Details of the formulation employed are provided in the article and the supplied electronic supplementary information includes details of all inputs and the results obtained for the Hemp cantilever and MBB beam examples described. Link: https://doi.org/10.15131/shef.data.14837913

## Disclosure statement

No potential conflict of interest was reported by the author(s).

## Funding

The financial support provided by Rolls-Royce plc is gratefully acknowledged. The work of M. Gilbert, A.G. Weldeyesus and J. Gondzio was financially supported by EPSRC [grant references EP/N023471/1 and EP/N019652/1].

## ORCID IDs

*S. J. Salt* https://orcid.org/0000-0002-5724-1628
*A. G. Weldeyesus* http://orcid.org/0000-0001-8696-8255
*M. Gilbert* https://orcid.org/0000-0003-4633-2839
*J. Gondzio* https://orcid.org/0000-0002-6270-4666

## References

Achtziger, W. 1999. "Local Stability of Trusses in the Context of Topology Optimization—Part I: Exact Modelling." *Structural Optimization* 17 (4): 235–246.
Achtziger, W., and M. Kočvara. 2007. "On the Maximization of the Fundamental Eigenvalue in Topology Optimization." *Structural and Multidisciplinary Optimization* 34 (3): 181–195.
Aroztegui, M., J. C. A. Costa Jr, A. Canelas, and J. Herskovits. 2011. "Maximising the Fundamental Frequency of Truss Structures." In *Proceedings of the 21st International Congress of Mechanical Engineering (COBEM 2011)*. Rio de Janeiro: Associação Brasileira de Engenharia e Ciências Mecânicas (ABCM).
Azad, S. K., M. Bybordiani, S. K. Azad, and F. Jawad. 2018. "Simultaneous Size and Geometry Optimization of Steel Trusses Under Dynamic Excitations." *Structural and Multidisciplinary Optimization* 58 (6): 2545–2563.
Ben-Tal, A., and A. Nemirovski. 1997. "Robust Truss Topology Design Via Semidefinite Programming." *SIAM Journal on Optimization* 7 (4): 991–1016.
Bendsøe, M. P., and O. Sigmund. 2003. *Topology Optimization: Theory, Methods and Applications*. Engineering Online Library. Berlin: Springer-Verlag. doi:10.1007/978-3-662-05086-6.
Cooper, D. A. 1989. "Report on the Accident to Boeing 737-400 G-OBME Near Kegworth Leicestershire on 8 January 1989." Technical Report. London, UK: Department of Transport. Air Accidents Investigation Branch; 1990. http://link.rbkc.gov.uk/portal/Report-on-the-accident-to-Boeing-737-400-G-OBME/9Yld5TQuZ7o/.
Desrosiers, J., and M. E. Lübbecke. 2005. *A Primer in Column Generation*, 1–32. Boston, MA: Springer US.
Dorn, W. S., R. E. Gomory, and H. J. Greenberg. 1964. "Automatic Design of Optimal Structures." *Journal de Mechanique* 3: 25–52.
Du, J., and N. Olhoff. 2007. "Topological Design of Freely Vibrating Continuum Structures for Maximum Values of Simple and Multiple Eigenfrequencies and Frequency Gaps." *Structural and Multidisciplinary Optimization* 34 (2): 91–110.
Fiala, J., M. Kočvara, and M. Stingl. 2013. "PENLAB: A MATLAB Solver for Nonlinear Semidefinite Optimization." ArXiv e-print, https://arxiv.org/pdf/1311.5240.pdf.
Fox, R. L., and M. P. Kapoor. 1970. "Structural Optimization in the Dynamics Response Regime—A Computational Approach." *AIAA Journal* 8 (10): 1798–1804.
Fujisawa, K., M. Fukuda, M. Kojima, and K. Nakata. 2000. *Numerical Evaluation of SDPA (Semidefinite Programming Algorithm)*, 267–301. Boston, MA: Springer US.
Gilbert, M., and A. Tyas. 2003. "Layout Optimization of Large-Scale Pin-Jointed Frames." *Engineering Computations* 20 (8): 1044–1064.
Giniūnaité, R. 2015. "Application of Semidefinite Programming to Truss Design Optimization." *Science—Future of Lithuania* 7 (3): 280–284.
Gondzio, J., P. González-Brevis, and P. Munari. 2013. "New Developments in the Primal–Dual Column Generation Technique." *European Journal of Operational Research* 224: 41–51.
Gondzio, J., and R. Sarkissian. 1996. *Column Generation with the Primal–Dual Method*. Technical Report 1996.4. CH-1211. Geneva, Switzerland: Logilab, University of Geneva.
Grandhi, R. V., and V. B. Venkayya. 1988. "Structural Optimization with Frequency Constraints." *AIAA Journal* 26 (7): 858–866.
Grant, M., and S. Boyd. 2014. "CVX: Matlab Software for Disciplined Convex Programming, Version 2.1." http://cvxr.com/cvx.
He, L., and M. Gilbert. 2015. "Rationalization of Trusses Generated Via Layout Optimization." *Structural and Multidisciplinary Optimization* 52 (4): 677–694.
He, L., M. Gilbert, and X. Song. 2019. "A Python Script for Adaptive Layout Optimization of Trusses." *Structural and Multidisciplinary Optimization* 60 (2): 835–847.
Hemp, W. S. 1973. *Optimum Structures*. Oxford, UK: Clarendon Press.

Kanno, Y. 2018. "Robust Truss Topology Optimization Via Semidefinite Programming with Complementarity Constraints: A Difference-of-Convex Programming Approach." *Computational Optimization and Applications* 71 (2): 403–433.

Kaveh, A., and M. Ilchi Ghazaan. 2016. "Optimal Design of Dome Truss Structures with Dynamic Frequency Constraints." *Structural and Multidisciplinary Optimization* 53 (3): 605–621.

Khot, N. S. 1985. "Optimization of Structures with Multiple Frequency Constraints." *Computers & Structures* 20 (5): 869–876.

Michell, A. G. M. 1904. "The Limits of Economy of Material in Frame-Structures." *Philosophical Magazine Series 6*, 8 (47): 589–597. doi:10.1080/14786440409463229.

MOSEK ApS. 2017. *MOSEK MATLAB Documentation Release 8.1.0.24*.

Parkes, E. W. 1975. "Joints in Optimum Frameworks." *International Journal of Solids and Structures* 11 (9): 1017–1022.

Pritchard, T. J., M. Gilbert, and A. Tyas. 2005. "Plastic Layout Optimization of Large-Scale Frameworks Subject to Multiple Load Cases, Member Self-Weight and with Joint Length Penalties." In *Proceedings of the 6th World Congress on Structural and Multidisciplinary Optimization*, Rio de Janeiro, 1–10. https://www.researchgate.net/publication/237133804.

Rozvany, G. I. N. 1998. "Exact Analytical Solutions for Some Popular Benchmark Problems in Topology Optimization." *Structural Optimization* 15 (1): 42–48.

Smith, C. J., M. Gilbert, I. Todd, and F. Derguti. 2016. "Application of Layout Optimization to the Design of Additively Manufactured Metallic Components." *Structural and Multidisciplinary Optimization* 54 (5): 1297–1313.

Sokół, T. 2014. "Multi-Load Truss Topology Optimization Using the Adaptive Ground Structure Approach." In *Recent Advances in Computational Mechanics*, edited by T. Łodygowski, J. Rakowski, and P. Litewka, 9–16. Boca Raton, FL: CRC Press.

Sokół, T., and G. I. N. Rozvany. 2013. "On the Adaptive Ground Structure Approach for Multi-Load Truss Topology Optimization." In *Proceedings of the 10th World Congress on Structural and Multidisciplinary Optimization*, Florida, 1–10. https://mae.ufl.edu/mdo/Papers/5428.pdf.

Taheri, Seyed Heja Seyed, and Shahin Jalili. 2016. "Enhanced Biogeography-Based Optimization: A New Method for Size and Shape Optimization of Truss Structures with Natural Frequency Constraints." *Latin American Journal of Solids and Structures* 13: 1406–1430.

Tejani, Ghanshyam G., Vimal J. Savsani, Vivek K. Patel, and Seyedali Mirjalili. 2018. "Truss Optimization with Natural Frequency Bounds Using Improved Symbiotic Organisms Search." *Knowledge-Based Systems* 143: 162–178.

Thore, C.-J. 2018. "FMINSDP—A Code for Solving Non-Linear Optimization Problems with Matrix Inequality Constraints." https://www.mathworks.com/matlabcentral/fileexchange/43643-fminsdp.

Tyburec, M., and J. Zeman. 2017. "Comparison of Semidefinite Solvers for Topology Optimization of Cantilever Trusses Subject to Fundamental Eigenvalue Constraint." *Advanced Materials Research* 1144: 172–177.

Weldeyesus, A. G., and J. Gondzio. 2018. "A Specialized Primal–Dual Interior Point Method for the Plastic Truss Layout Optimization." *Computational Optimization and Applications* 71 (3): 613–640.

Weldeyesus, A. G., J. Gondzio, L. He, M. Gilbert, P. Shepherd, and A. Tyas. 2019. "Adaptive Solution of Truss Layout Optimization Problems with Global Stability Constraints." *Structural and Multidisciplinary Optimization* 60 (5): 2093–2111.

Wolkowicz, H., R. Saigal, and L. Vandenberghe. 2000. *Handbook of Semidefinite Programming. Theory, Algorithms, and Applications*. Dordrecht, The Netherlands: Kluwer Academic.